

Supplementary Information

for

**Efficient Photochemical Water Oxidation by a
Dinuclear Molecular Ruthenium Complex**

Tanja M. Laine,^[a] Markus D. Kärkäs,^{[a]} Rong-Zhen Liao,^{[a]*} Torbjörn Åkermark,^[a] Bao-Lin Lee,^[a]
Erik A. Karlsson,^[a] Per E. M. Siegbahn,^[a] and Björn Åkermark^{[a]*}*

[a] Department of Organic Chemistry, Arrhenius Laboratory, Stockholm University, SE-106 91
Stockholm, Sweden

Email: markusk@organ.su.se, rongzhen@organ.su.se, bjorn.akermark@organ.su.se

Experimental Details

Materials and methods. $\text{Ru}(\text{DMSO})_4\text{Cl}_2$,^[S1] and $[\text{Ru}(\text{bpy})_3](\text{PF}_6)_3$ ^[S2] were prepared according to previously reported procedures. $[\text{Ru}(\text{bpy})_3]\text{Cl}_2$ was obtained from TCI and used without additional purification. All other reagents including solvents were obtained from Sigma-Aldrich and used directly without further purification. All solvents were dried by standard methods when needed. Column chromatography was performed on silica gel (Grace Division, Davsil, 0.035-0.070 mm). ^1H and ^{13}C NMR spectra were recorded at 400 MHz and at 100 MHz, respectively, if not otherwise stated. Chemical shifts (δ) are reported in ppm, using the residual solvent peak [$[\text{D}_6]$ DMSO ($\delta(\text{H}) = 2.50$ and $\delta(\text{C}) = 39.52$); $[\text{D}_4]$ methanol ($\delta(\text{H}) = 3.31$); CDCl_3 ($\delta(\text{H}) = 7.26$ and $\delta(\text{C}) = 77.16$)] as internal standard. Splitting patterns are assigned as s (singlet), d (doublet), t (triplet), q (quartet), m (multiplet), and br (broad). High resolution mass spectrum measurements were recorded on a Bruker Daltonics microTOF spectrometer with an electrospray ionizer. IR spectra were recorded on a Perkin-Elmer Spectrum One spectrometer, using solid sample prepared as KBr discs. EPR spectra were recorded at 77K on a Varian E9 spectrometer equipped with a quartz insert for liquid nitrogen. Measurements were made with a microwave frequency of 9.12GHz, a microwave power of 8 mW and a modulation amplitude of 2mT. Elemental analyses were carried out at MEDAC Ltd, Chobham, Surrey, United Kingdom.

Electrochemistry. Electrochemical measurements were carried out with an Autolab potentiostat with a GPES electrochemical interface (Eco Chemie), using a glassy carbon disk (diameter 3 mm) as the working electrode, and platinum as the counter-electrode. The reference electrode was a saturated calomel electrode (SCE). All potentials reported herein are converted to normal hydrogen electrode (NHE) by using the $[\text{Ru}(\text{bpy})_3]^{3+}/[\text{Ru}(\text{bpy})_3]^{2+}$ couple ($E_{1/2} = 1.26$ V vs. NHE) as reference. The electrolytes used were either an aqueous phosphate buffer solution (0.1 M, pH 7.2), an aqueous phosphoric acid solution (0.1 M, pH 1.0) or an aqueous triflic acid solution (0.1 M, pH 1.0).

Gas evolution measurements. Oxygen evolution was measured by mass spectrometry (MS). The mass spectrometer consists of three separate parts connected with gas valves. These parts are a reaction chamber, a Gas Handling System (GHS), and a mass spectrometer (MKS Spectra Products, Microvision Plus, 0-100 mass units) in Ultra High Vacuum (base pressure $2 \cdot 10^{-10}$ mbar). The GHS makes it possible to control the atmosphere in the enclosed volume. A rough pump is used to evacuate the GHS, so the pressure can be regulated within 0.1-1000 mbar. With this setup, the enclosed volume in the reaction chamber is continuously probed by the mass spectrometer by an inlet through the leak valve. The inlet to the mass spectrometer is so small that the probing causes a negligible pressure change in the enclosed volume. This means that the measurements do not influence the reaction rates measured.

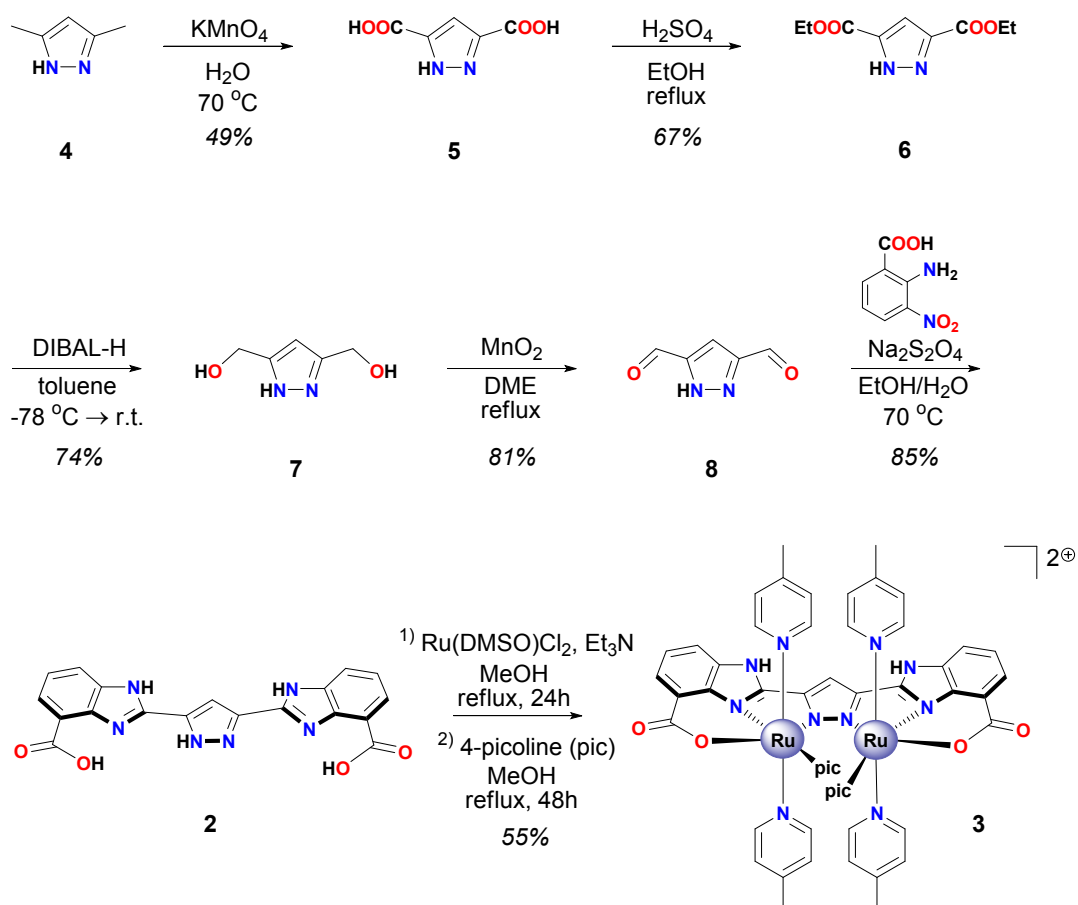
The change with time of the measured pressure of masses 0-100 in the MS can be converted to the amount in the enclosed volume in two steps. The first step is to convert the pressure in the MS to the pressure in the enclosed volume. This conversion is done by calibration of the system, *i.e.* measuring the response in the MS to different pressures in the enclosed volume. In the second step the pressures in the enclosed volume are converted to the amounts of the different gases. This makes it possible to determine the evolution of gases with masses 1-100 quantitatively. A ca 1 cm thick rubber gasket has been added to the system. This permits injection of solutions containing reactants into the reaction chamber, essentially without leaking in of the external atmosphere. Any leakage of air is continuously measured with the MS (increase of both O₂ and N₂).

A stock solution was made of the catalyst in H₃PO₄. The catalyst solutions used in the experiments were then made by diluting the stock solutions with phosphate buffer (0.1 M, pH 7.2) to the desired concentrations. The solutions were then deoxygenated by bubbling with N₂ for at least 15 min before being used in the experiments. In a typical run, [Ru(bpy)₃](PF₆)₃ (3.0 mg, 3.0 μmol) was placed in the reaction chamber and the reaction chamber was evacuated with a rough pump. ~40 mbar He was then introduced into the system. After a couple of minutes the catalyst solution (0.50 mL) was injected into the reaction chamber. The evolved oxygen gas was then measured and recorded versus time by MS.

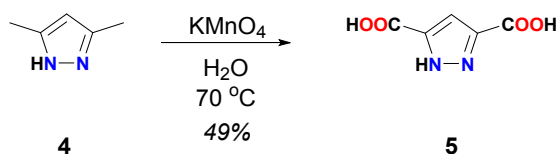
¹⁸O-Isotopic experiments. An aqueous phosphate buffer solution (0.1 M, pH 7.2, 0.50 mL, 8.7% H₂¹⁸O) containing catalyst **3** (3.0 μM), bubbled with N₂ for 15 min, was added to [Ru(bpy)₃](PF₆)₃ (3.1 mg, 3.1 μmol) in the reaction chamber. The evolved oxygen gas was measured and recorded versus time by MS.

Computational details. The geometry optimizations in the present study were performed using the Gaussian 09^[S3] package and the B3LYP^[S4] functional. The 6-31G(*d,p*) basis set was applied for the C, N, O, H elements and the SDD^[S5] pseudopotential for Ru. Frequencies were calculated analytically at the same level of theory as the geometry optimization to obtain the Gibbs free energy corrections and to confirm the nature of various stationary points. Solvation effects from the H₂O solvent were calculated using the SMD^[S6] continuum solvation model with the larger basis set where all elements, except Ru, were described by 6-311+G(2*df*,2*p*) at the B3LYP* (15% exact exchange) level.^[S7] It has been shown that B3LYP* gives a better description of relative energies in transition metal complexes.^[S7] For calculating pK_a values, the gas phase Gibbs free energy of a proton is -6.3 kcal mol⁻¹ and the experimental solvation free energy of the proton (-264.0 kcal mol⁻¹) was used.^[S8] Unless otherwise specified, the B3LYP*-D2 energies are reported, including Gibbs free energy corrections from B3LYP and dispersion corrections proposed by Grimme.^[S9]

Synthesis

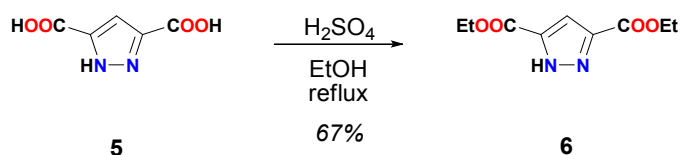


Scheme S1. Synthesis and structures of ligand **2** and molecular Ru complex **3**.

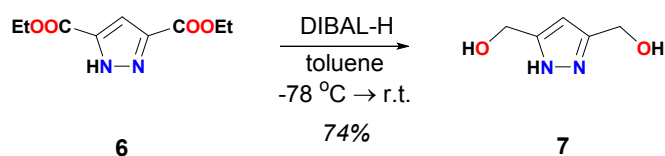


Synthesis of 1H-pyrazole-3,5-dicarboxylic acid (5). 3,5-dimethyl-pyrazole **4** (22.0 g, 0.229 mol) was suspended in H₂O (180 mL), in a beaker with a mechanical stirrer. The suspension was heated to 70 °C, after which KMnO₄ (187 g, 1.19 mol) was added portion-wise to the solution. The temperature of the reaction mixture was kept between 85 and 95 °C. An excess of KMnO₄ (6 x 7.0 g) was gradually added as the oxidant was consumed. The hot mixture was filtered after 2 h and washed with hot H₂O (~200 mL). The pH of the filtrate was adjusted to pH 1 with concentrated HCl (~60 mL). The white precipitate was collected after approximately 2 days and washed with ice-cold H₂O (~40 mL), after

which it was dried over vacuum to afford compound **5** as a white solid (17.6 g, 49 %). ¹H NMR (D₂O, 400 MHz): δ (ppm) = 7.53 (s, 1H); ¹³C NMR (D₂O, 100 MHz, 50 °C, with dioxane as internal standard): δ (ppm) = 164.2, 141.4, 111.6; HRMS (ESI) Calcd. for C₅H₃N₂O₄ [M - H]⁻: 155.0098; found: 155.0100.

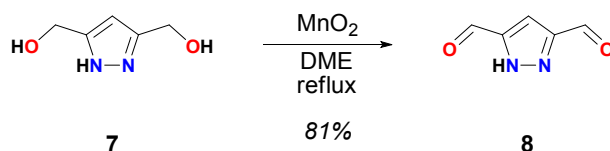


Synthesis of diethyl 1H-pyrazole-3,5-dicarboxylate (6).^[S10] Compound **5** (1.00 g, 6.40 mmol) was suspended in EtOH (50 mL). The suspension was cooled to 0 °C, after which concentrated H₂SO₄ (5 mL) was added drop-wise. The reaction mixture was refluxed for 48 h, after which the solvent was evaporated. The resulting mixture was diluted with H₂O (~100 mL) and extracted with CH₂Cl₂ (3 x 125 mL). The organic layer was dried over Na₂SO₄ and evaporated. The oily product was purified by flash column chromatography (Et₂O/pentane, 2:1) to afford **6** as a white solid (0.90 g, 67 %). ¹H NMR (CDCl₃, 400 MHz): δ (ppm) = 11.23 (s, 1H), 7.34 (s, 1H), 4.42 (q, *J* = 7.14 Hz, 4H), 1.41 (t, *J* = 7.14 Hz, 6H); ¹³C NMR (CDCl₃, 100 MHz): δ (ppm) = 160.5, 139.9, 111.4, 61.8, 14.3; HRMS (ESI) Calcd. for C₉H₁₃N₂O₄ [M + H]⁺: 213.0870; found: 213.0863.

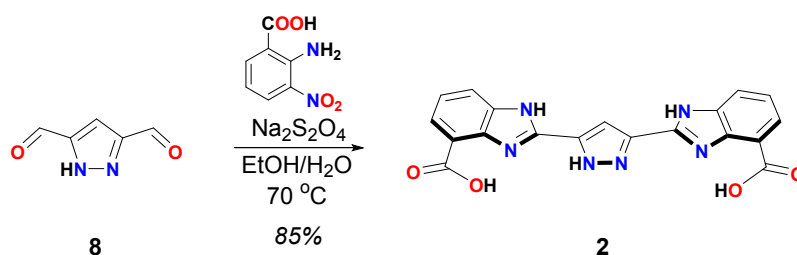


Synthesis of 3,5-bis(hydroxymethyl) pyrazole (7).^[S10] Compound **6** (0.620 g, 2.90 mmol) was dissolved in toluene (4.4 mL). The solution was cooled to -78 °C, after which DIBALH (17.6 mL, 17.6 mmol) was added drop-wise over 25 min. After stirring the reaction mixture at -78 °C overnight the mixture was run at r.t for ~24 h. The solution was cooled to 0 °C, after which MeOH (100 mL) was added drop-wise. The white precipitate was collected and dried under reduced pressure. The solid was subsequently extracted with MeOH in a Soxhlet apparatus for 4 days. Evaporation of the solvent gave a yellow oil, which after trituration with EtOAc afforded the product as a white solid (0.28 g, 74

%). ¹H NMR ([D₆]DMSO, 400 MHz): δ (ppm) = 12.36 (bs, 1H), 6.07 (s, 1H), 5.02 (bs, 2H), 4.40 (s, 4H); ¹³C NMR ([D₆]DMSO, 100 MHz): δ (ppm) = 140.3, 93.7, 48.0; HRMS (ESI) Calcd. for C₅H₈N₂O₂Na [M + Na]⁺: 151.0478; found: 151.0479.

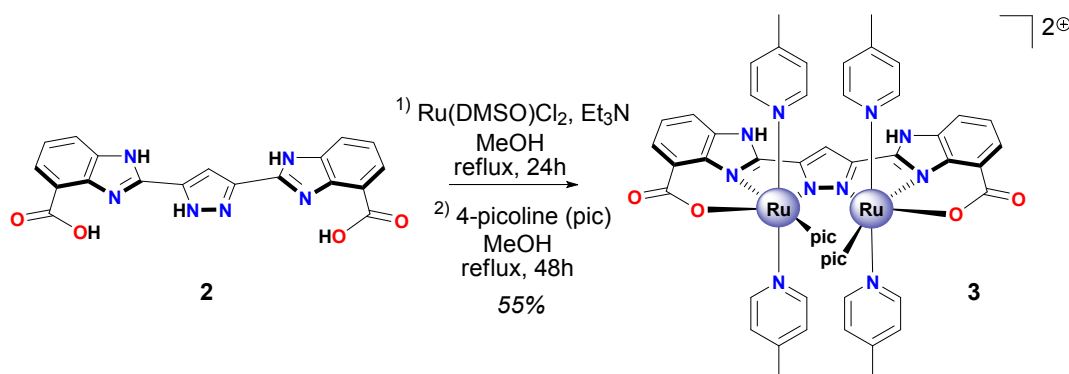


Synthesis of 1H-pyrazole-3,5-dicarbaldehyde (8).^[S10] MnO₂ (2.20 g, 26.0 mmol) was added portion-wise to a refluxing solution of dimethoxyethane (DME) (56 mL) containing compound **7** (0.290 g, 2.20 mmol). The reaction mixture was refluxed for 3 h after which the hot mixture was filtered over Celite and washed with hot MeOH (3 x 20 mL). Charcoal was added to the filtrate, filtered over Celite and again washed with hot MeOH (3 x 20 mL). The filtrate was evaporated to dryness and recrystallized from *i*-PrOH to afford the title compound as a white solid (0.22 g, 81 %). ¹H NMR ([D₆]DMSO, 400 MHz, 80 °C): δ (ppm) = 14.90 (bs, 1H), 9.94 (s, 2H), 7.50 (s, 1H); ¹³C NMR ([D₆]DMSO, 100 MHz, 80 °C): δ (ppm) = 183.5, 147.0, 109.5; HRMS (ESI) Calcd. for C₅H₃N₂O₂ [M - H]⁺: 123.0200; found: 123.0212.



Synthesis of 3,5-bis(4-carboxy-1H-benzimidazol-2-yl)-1H-pyrazole (2, H₅L). Compounds **8** (0.100 g, 0.820 mmol) and 2-amino-3-nitrobenzoic acid (0.300 g, 1.64 mmol) were suspended in EtOH (3.3 mL). An aqueous solution of sodium dithionite (0.860 g, 4.90 mmol, 4.90 mL) was added to the suspension, after which the reaction mixture was heated to 70 °C for 5 h. The dark yellow precipitate was collected by filtration and washed with H₂O and EtOH to afford the title compound as a dark yellow solid (0.27 g, 85 %). ¹H NMR (D₂O containing 3 equiv. K₃PO₄, 400 MHz): δ (ppm) = 7.79 (d,

$J = 7.90$ Hz, 2H), 7.72 (d, $J = 7.50$ Hz, 2H), 7.48 (s, 1H), 7.32 (t, $J = 7.70$ Hz, 2H); ^{13}C NMR ($[\text{D}_6]\text{DMSO}$, 500 MHz, 40 °C): δ (ppm) = 167.9, 145.6, 142.6, 135.5, 124.3, 121.6, 121.4, 118.3, 105.3; HRMS (ESI) Calcd. for $\text{C}_{19}\text{H}_{11}\text{N}_6\text{O}_4$ $[\text{M} - \text{H}]^-$: 387.0847; found: 387.0866.



Synthesis of Ru complex 3(PF₆)₂ ([$(\text{H}_2\text{L})\text{Ru}_2(\text{pic})_6$](PF₆)₂). Ligand **2** (60.0 mg, 0.160 mmol) and Et₃N (0.30 mL) were added to MeOH (6.0 mL). After bubbling the suspension in Ar for 10 min Ru(DMSO)₄Cl₂ (0.150 g, 0.310 mmol) was added and the reaction mixture was refluxed for 24 h. 4-Picoline (0.150 mL, 1.54 mmol) was added to the reaction mixture and the mixture was further refluxed for 48 h. The green crude reaction mixture was evaporated to dryness and added to an aqueous sat. KPF₆ solution (30 mL). The resulting dark-green precipitate was filtered and washed with H₂O (3 x 10 mL) and Et₂O (2 x 10 mL) by centrifugation to yield complex **3** (140 mg, 55.4 %). HRMS (ESI) Calcd. for $\text{C}_{55}\text{H}_{50}\text{N}_{12}\text{O}_4\text{Ru}_2$ [**3** - H]⁺: 1146.2159; found: 1146.2196; Anal. calcd. for $\text{C}_{59}\text{H}_{67}\text{F}_{12}\text{N}_{12}\text{O}_8\text{P}_2\text{Ru}_2\text{S}_2$ [**3**(PF₆)₂ · 2H₂O · 2(CH₃)₂SO]: C 43.52, H 4.15, N 10.32, S 3.94 %; found: C 43.91, H 4.15, N 10.27, S 3.78 %; IR (KBr disc): ν_{max} = 3422, 2923, 2853, 1942, 1620, 1559, 1500, 1424, 1369, 1209, 1062, 1034, 814, 762, 727, 677, 636, 503, 470.

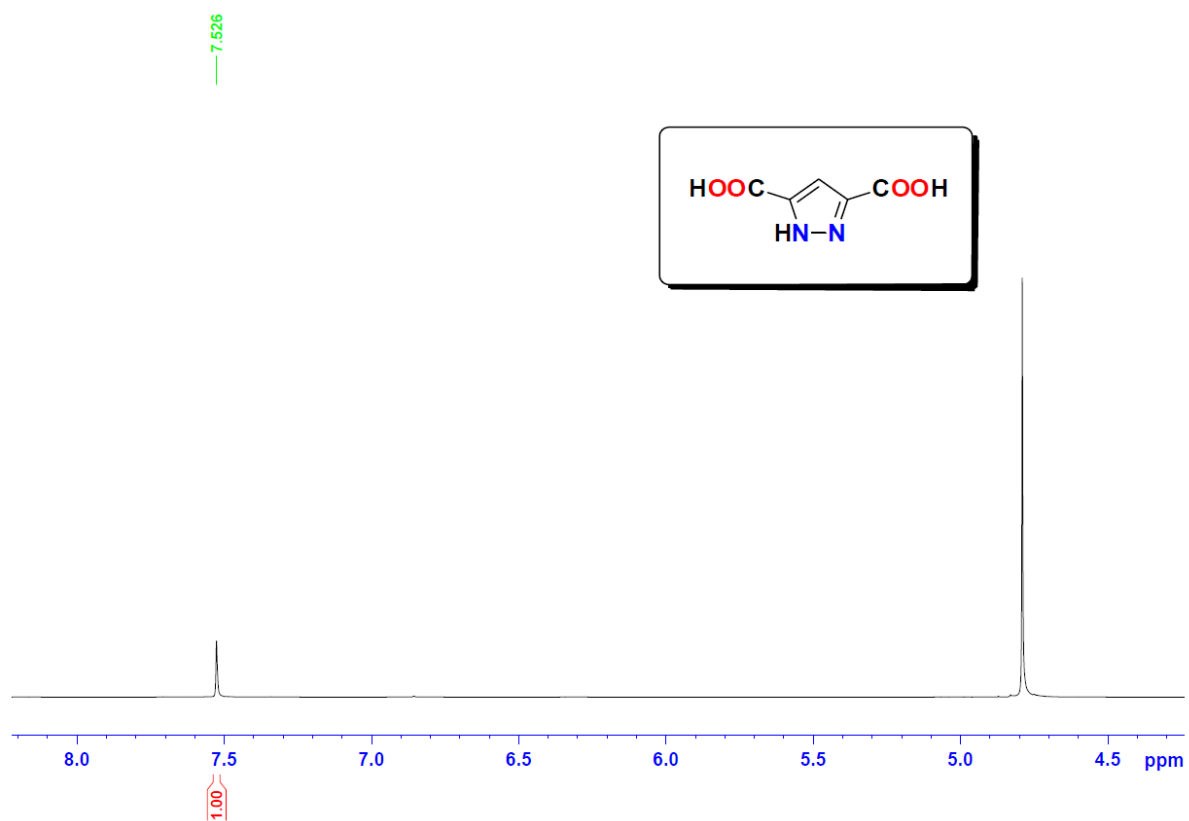


Figure S1. ¹H NMR spectrum of diacid **5** in D₂O.

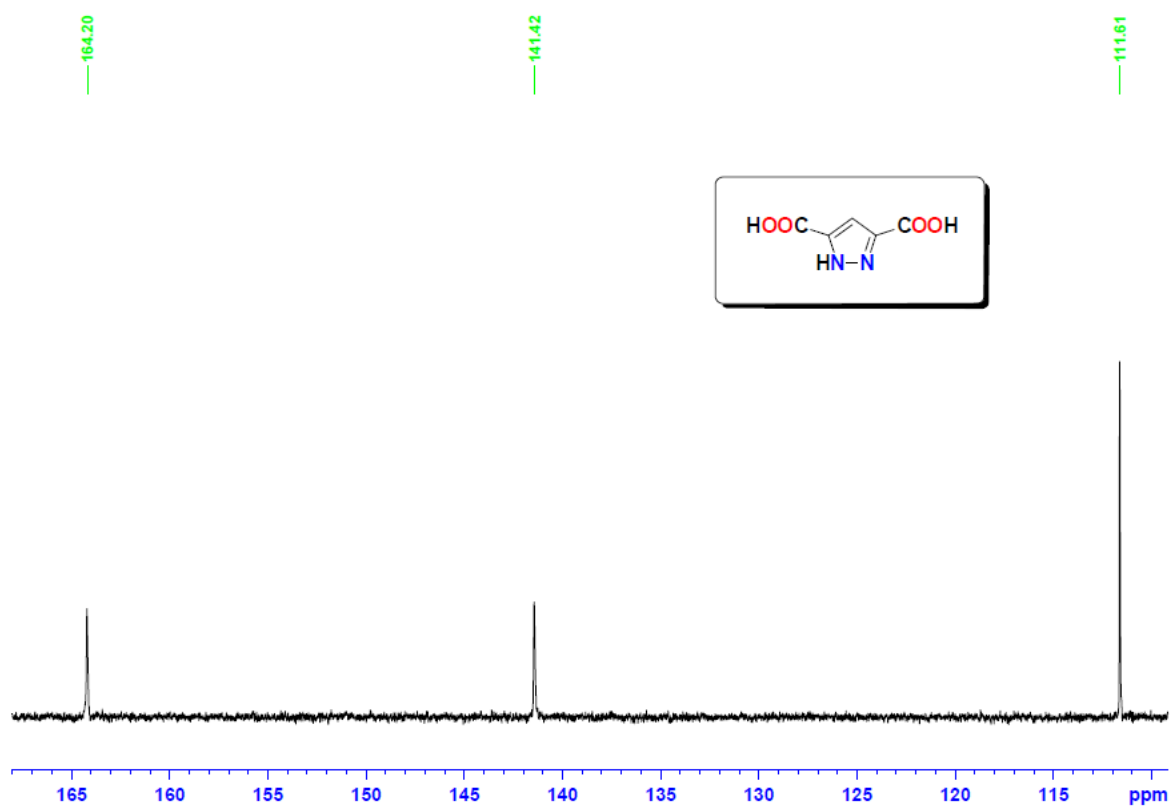


Figure S2. ^{13}C NMR spectrum of diacid **5** in D_2O .

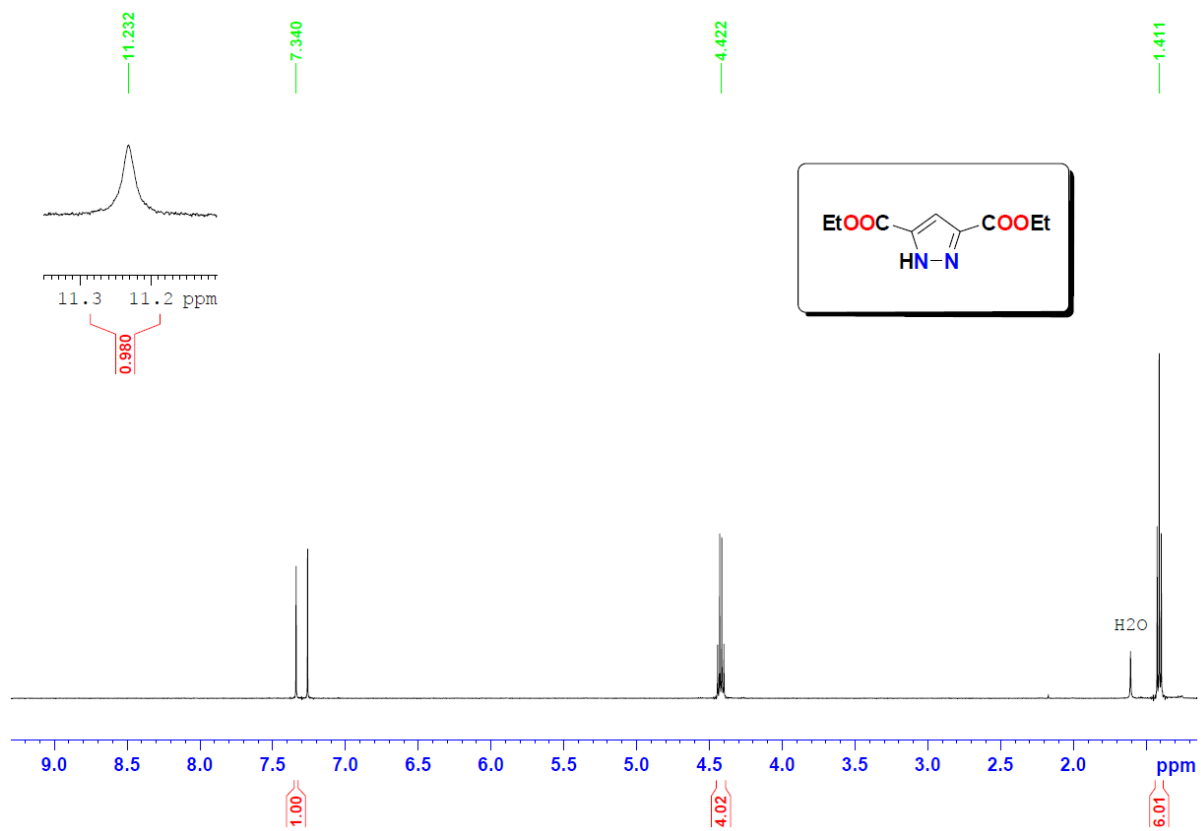


Figure S3. ^1H NMR spectrum of diester **6** in CDCl_3 .

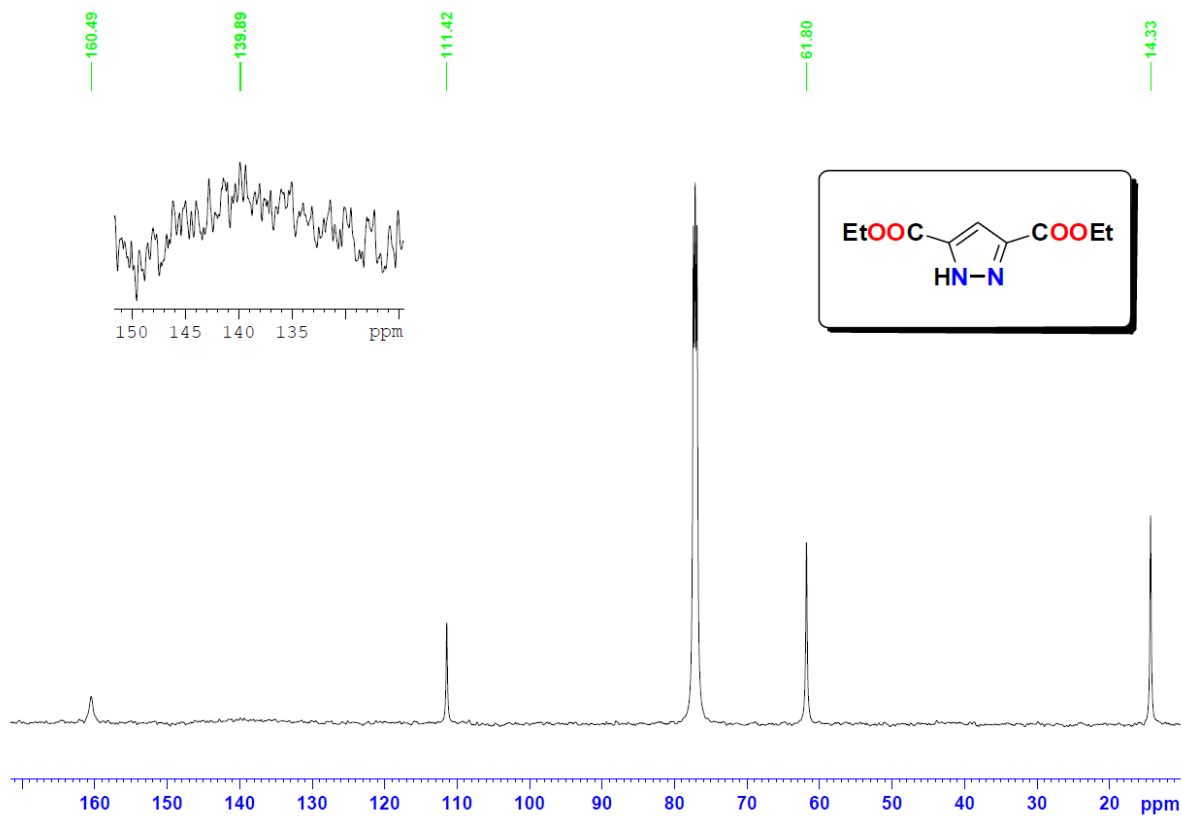


Figure S4. ¹³C NMR spectrum of diester **6** in CDCl₃

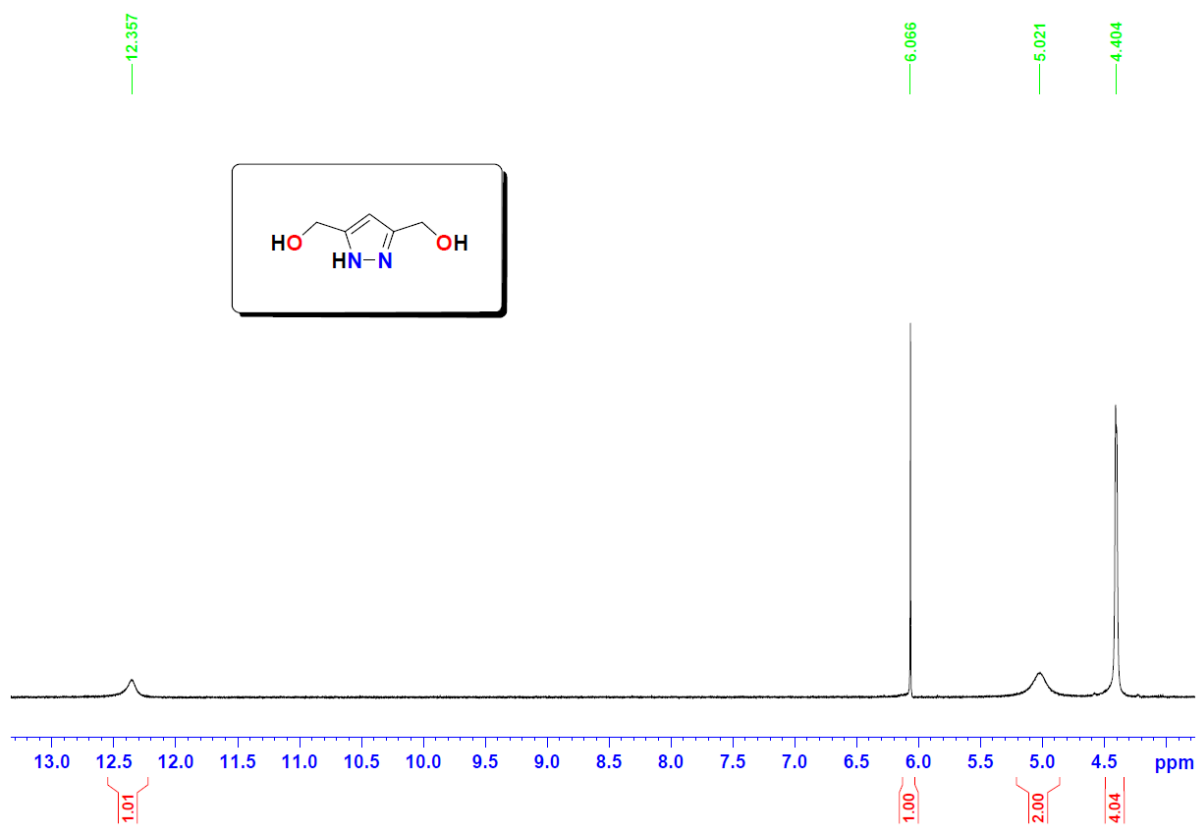


Figure S5. ^1H NMR spectrum of diol **7** in $[\text{D}_6]\text{DMSO}$.

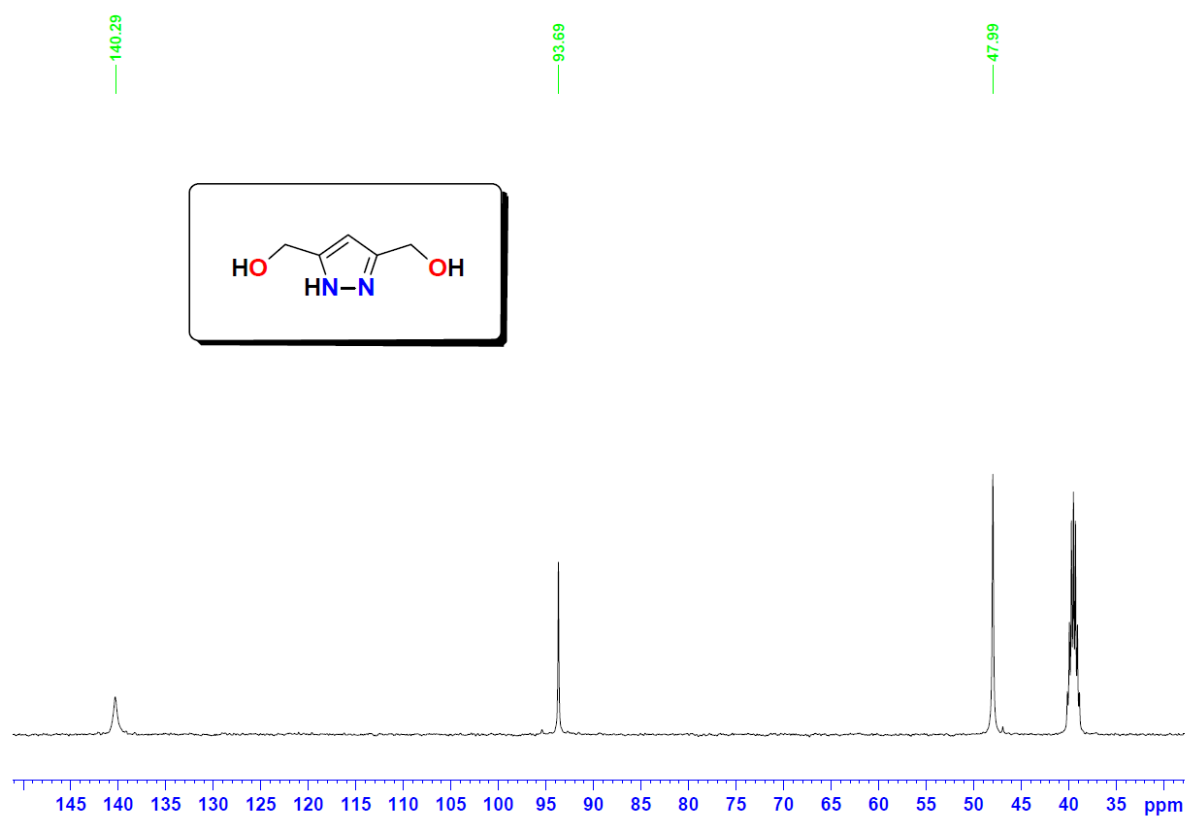


Figure S6. ^{13}C NMR spectrum of diol **7** in $[\text{D}_6]\text{DMSO}$.

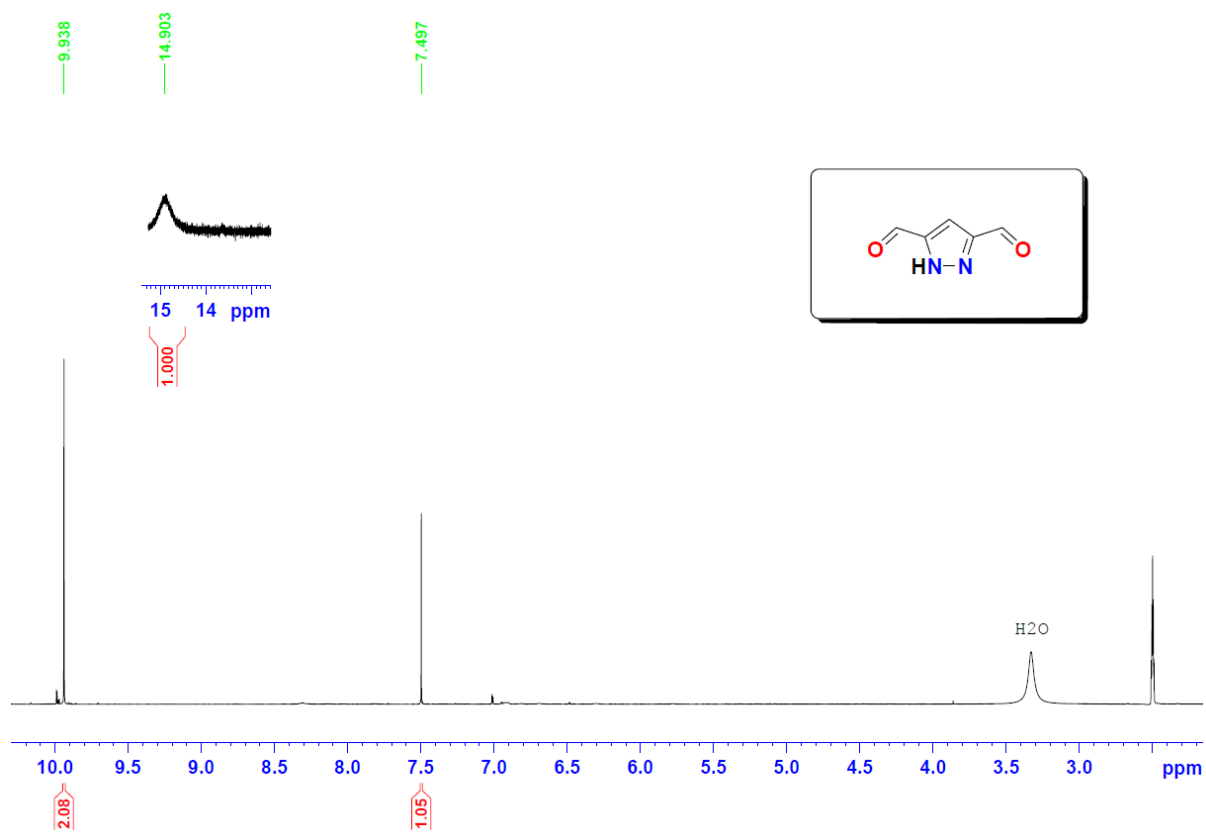


Figure S7. ^1H NMR spectrum of dialdehyde **8** in $[\text{D}_6]\text{DMSO}$.

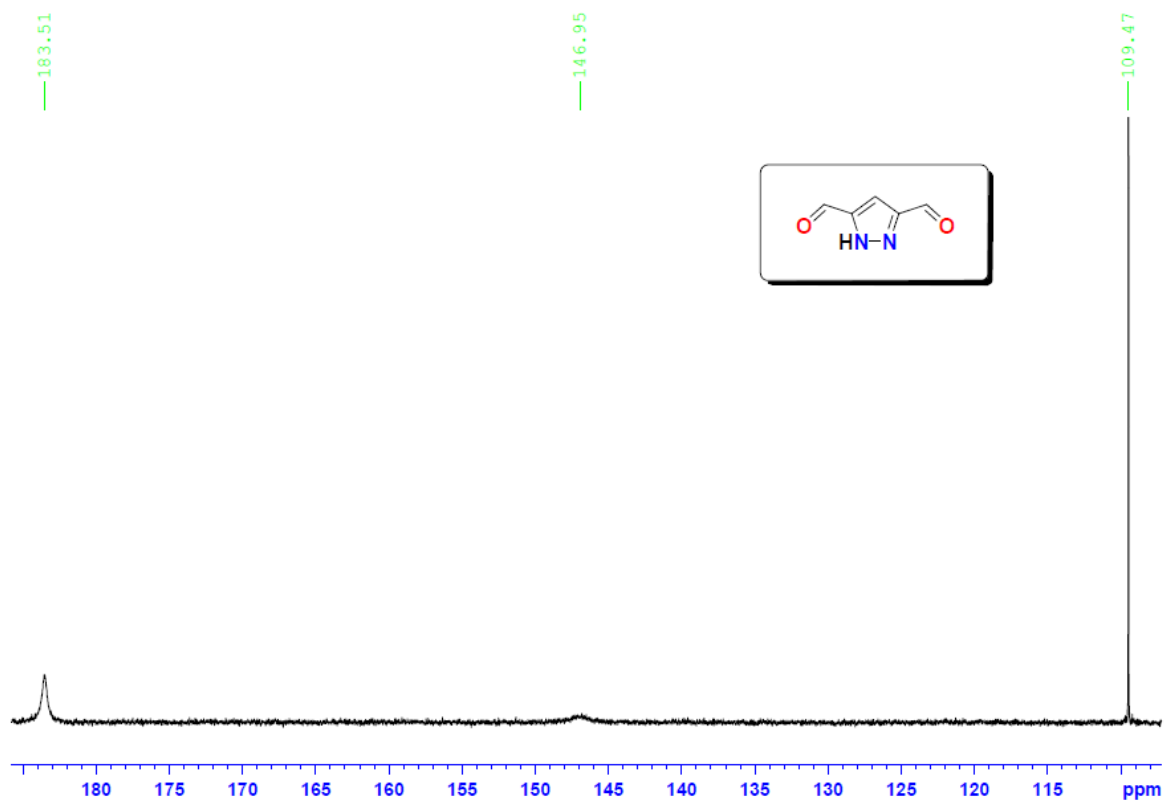


Figure S8. ^{13}C NMR spectrum of dialdehyde **8** in $[\text{D}_6]\text{DMSO}$.

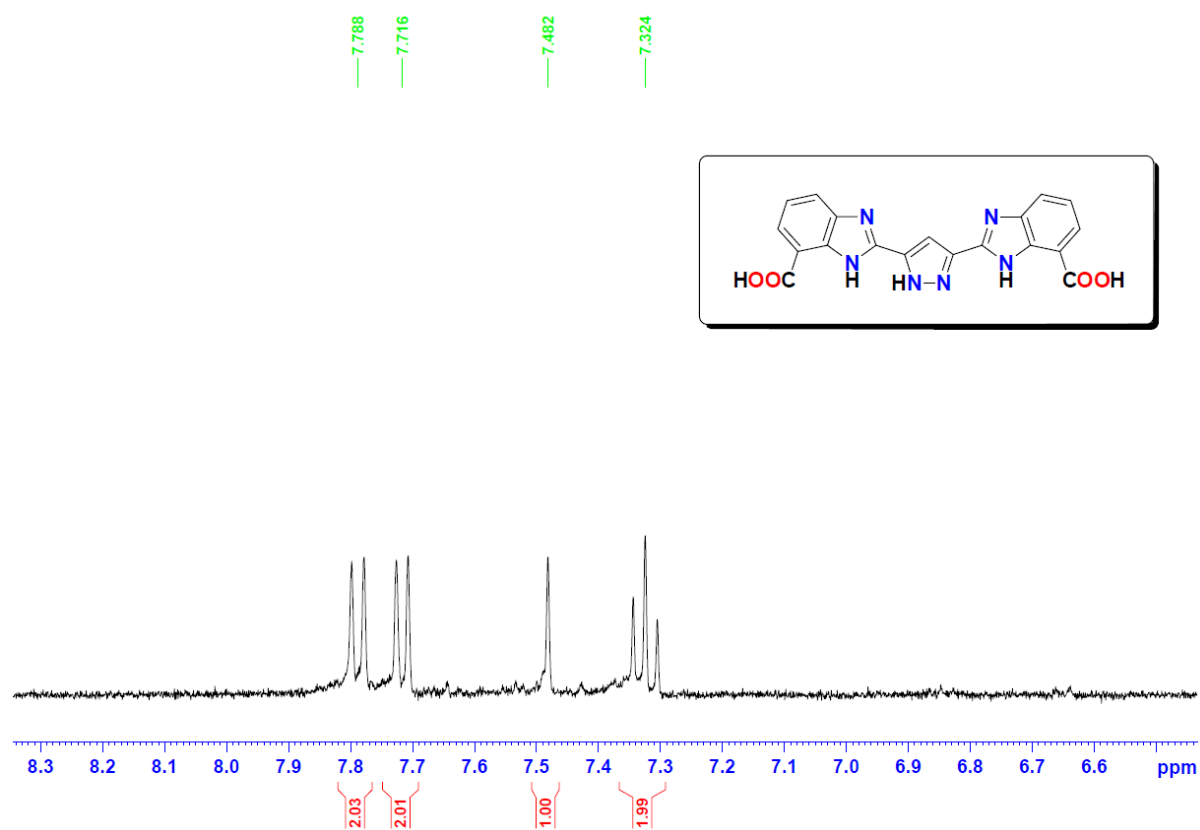


Figure S9. ^1H NMR spectrum of ligand **2** in D_2O containing 3 equivalents K_3PO_4 .

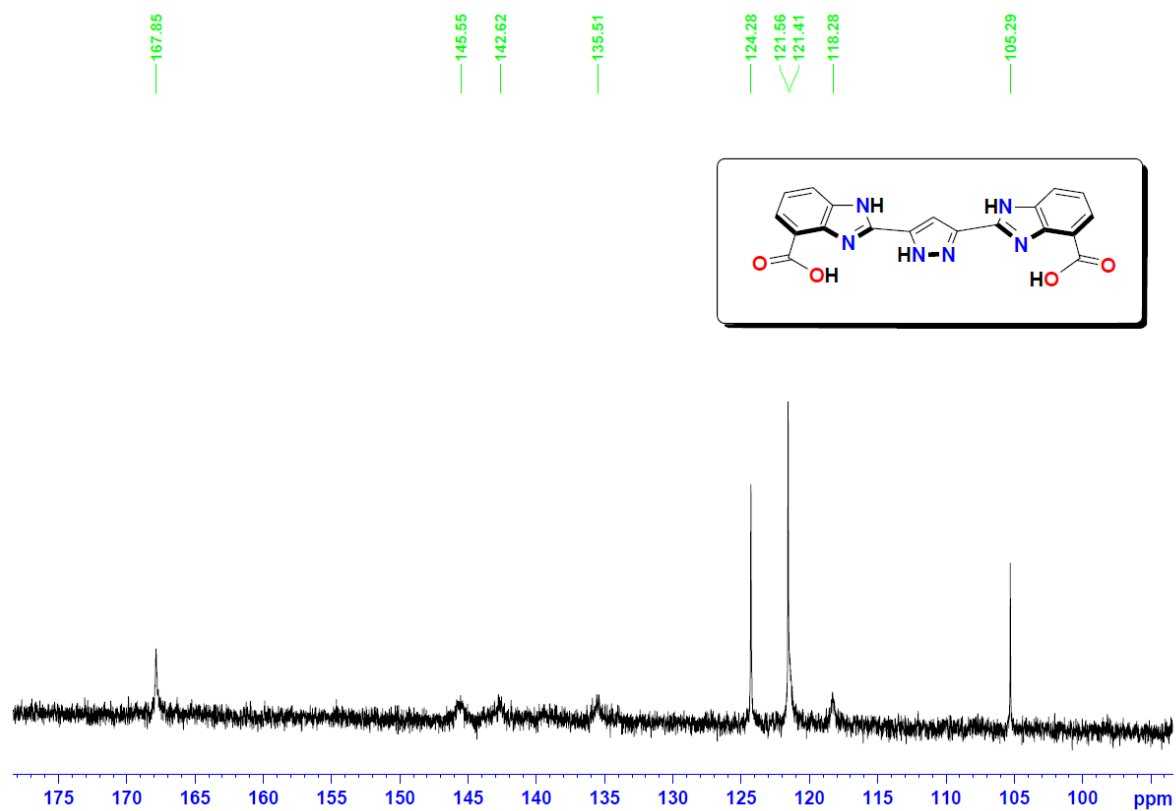


Figure S10. ^{13}C NMR spectrum of ligand **2** in $[\text{D}_6]\text{DMSO}$.

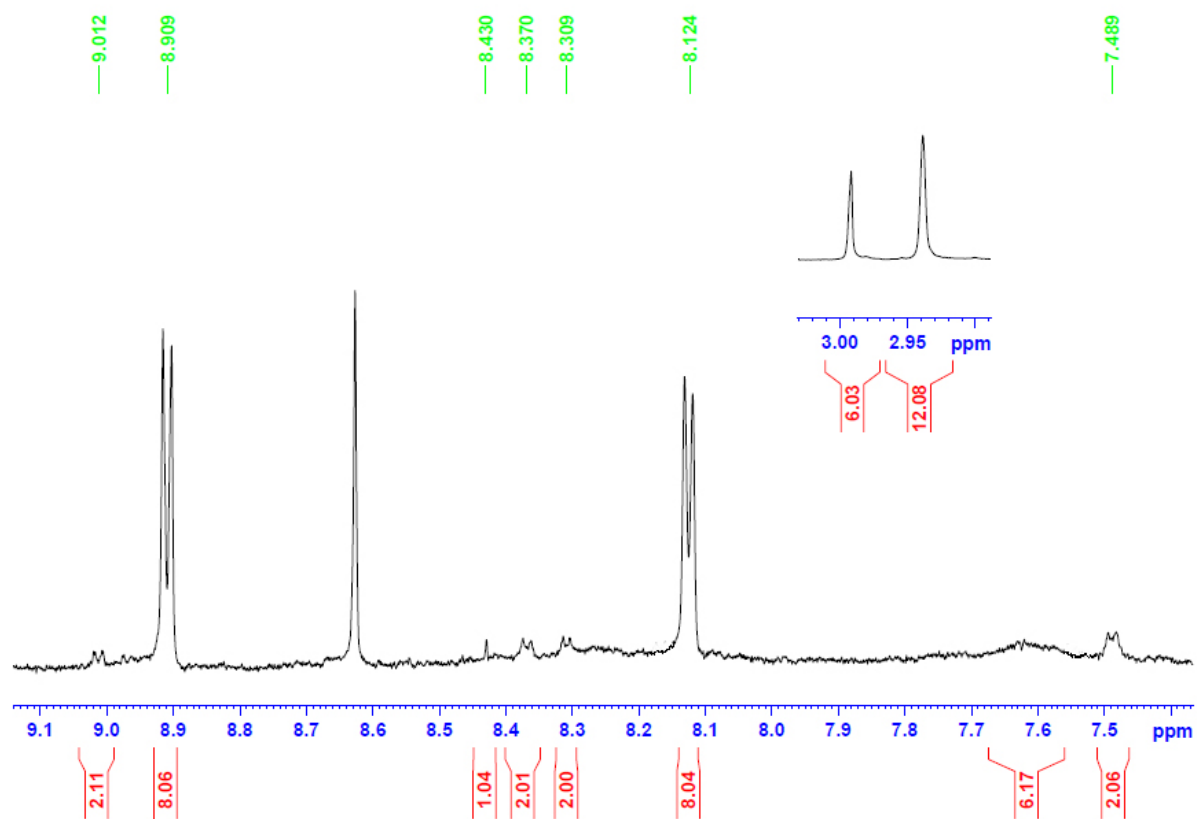


Figure S11. ^1H NMR spectrum of Ru complex **3** in $[\text{D}_4]\text{MeOH}/\text{D}_2\text{O}$ (1:1) at 50 °C containing 30 equivalents $\text{Na}_2\text{S}_2\text{O}_4$.

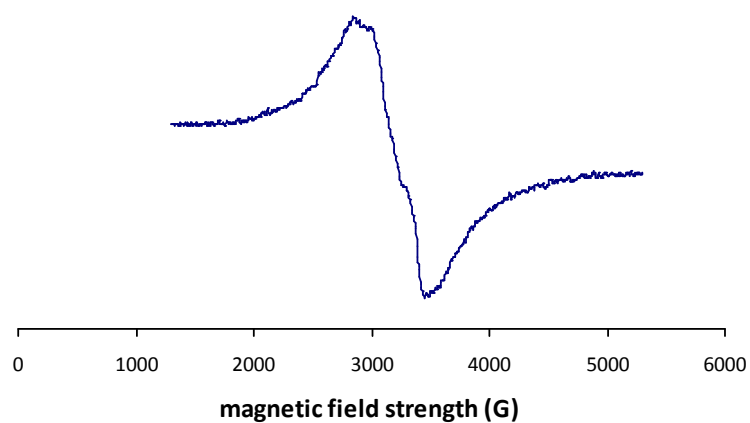


Figure S12. Solid state EPR-spectra of Ru complex **3**.

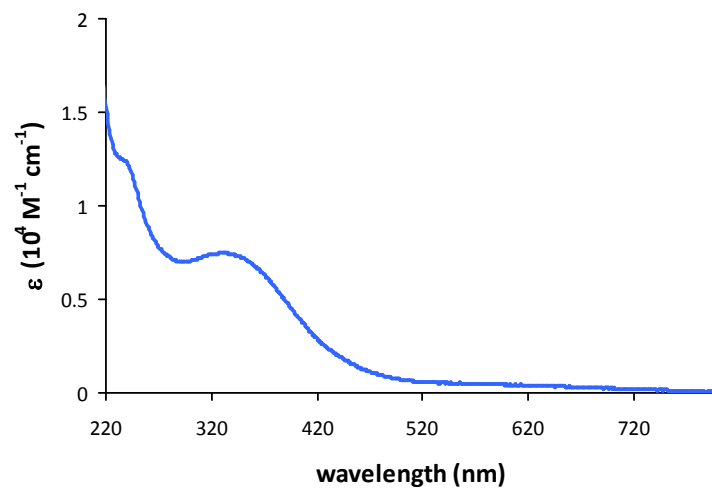


Figure S13. UV-vis spectrum of Ru complex **3** in an aqueous phosphate buffer solution (0.1 M, pH 7.2).

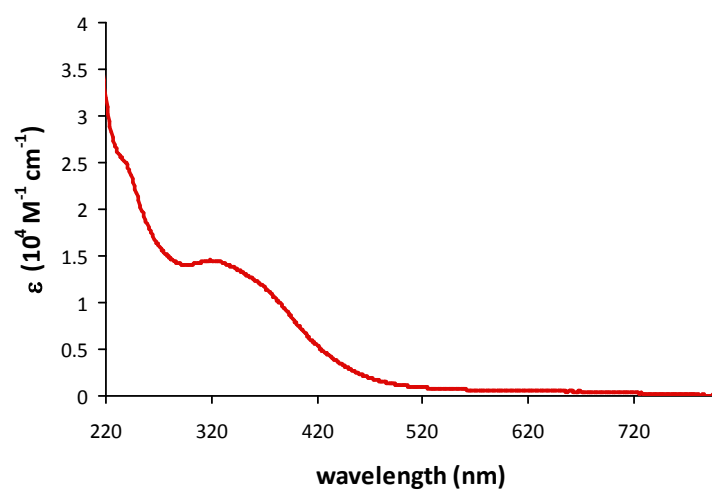


Figure S14. UV-vis spectrum of Ru complex **3** in an aqueous H_3PO_4 solution (0.1 M, pH 1.0).

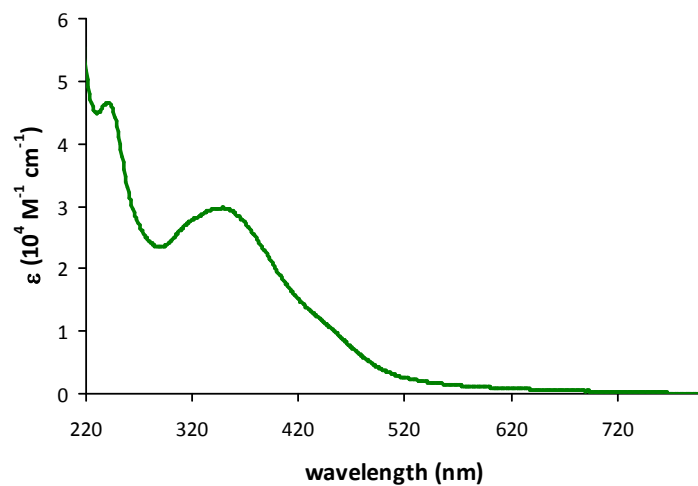


Figure S15. UV-vis spectrum of Ru complex **3** in a MeOH solution.

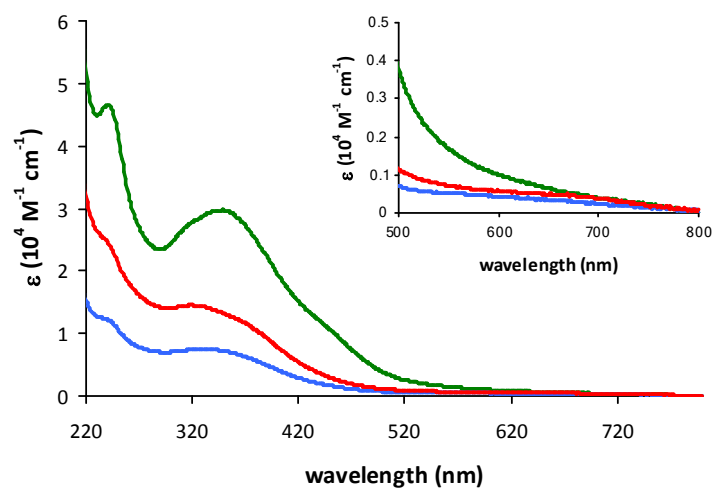


Figure S16. UV-vis spectra of Ru complex **3** in (—) an aqueous phosphate buffer solution (0.1 M, pH 7.2), (—) in an aqueous H_3PO_4 solution (0.1 M, pH 1) and (—) in a MeOH solution.

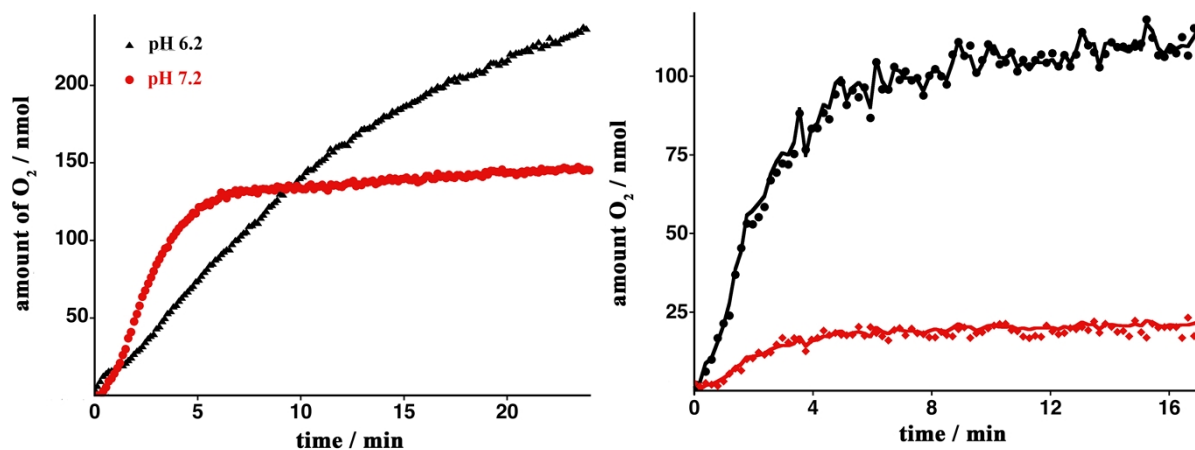


Figure S17. Left: Chemical H₂O oxidation catalyzed by dinuclear Ru complex **3** at pH 6.2 and 7.2, using [Ru(bpy)₃]³⁺ as the chemical oxidant. Reaction conditions: An aqueous phosphate buffer solution (0.1 M, 0.50 mL) containing Ru complex **3** (0.60 μM) was added to the oxidant [Ru(bpy)₃](PF₆)₃ (3.0 mg, 3.0 μmol). Right: Chemical H₂O oxidation catalyzed by Ru complex **3** in isotopically labeled H₂O (8.7% H₂¹⁸O). Reaction conditions: An aqueous phosphate buffer solution (0.1 M, pH 7.2, 0.50 mL, 8.7% H₂¹⁸O) containing catalyst **3** (3.0 μM) was added to the oxidant [Ru(bpy)₃](PF₆)₃ (3.0 mg, 3.0 μmol). ^{16,16}O₂ measured (▲), ^{16,18}O₂ measured (●).

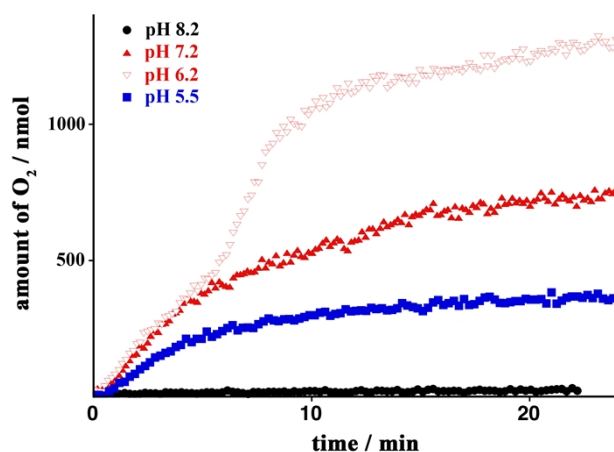


Figure S18. Photochemical H₂O oxidation catalyzed by Ru complex **3** at various pH. Reaction conditions: Reactions were performed in an aqueous phosphate buffer solution (0.1 M, 0.50 mL) containing Ru complex **3** (3.0 μM), [Ru(bpy)₂(deeb)](PF₆)₂ as photosensitizer (0.60 mM) and Na₂S₂O₈ as sacrificial electron acceptor (23.5 mM).

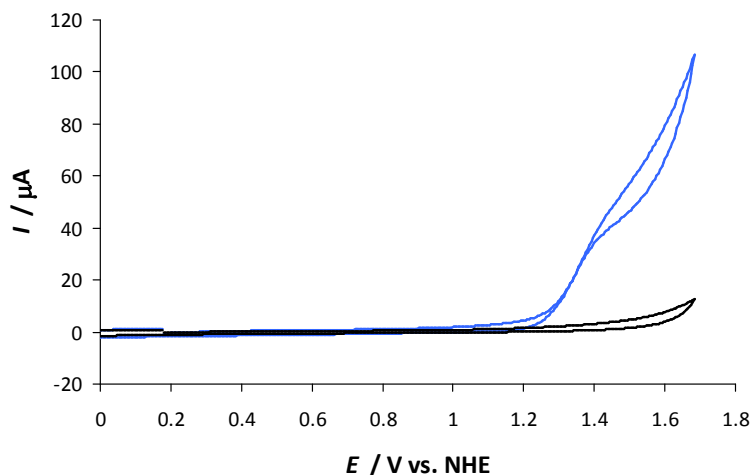
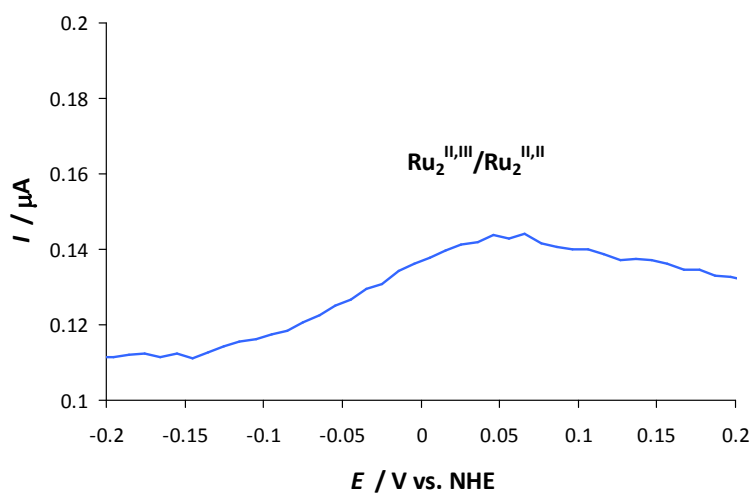


Figure S19. Cyclic voltammograms of (—) Ru complex **3** in an aqueous phosphate buffer solution (pH 7.2) and of (—) phosphate buffer (pH 7.2) in the absence of Ru complex **3**. Conditions: Voltammograms were recorded in an aqueous phosphate buffer solution (0.1 M, pH 7.2) containing complex **3** (60 μM) with a scan rate of 0.1 V s⁻¹, using the $[\text{Ru}(\text{bpy})_3]^{3+}/[\text{Ru}(\text{bpy})_3]^{2+}$ couple as a standard ($E_{1/2} = 1.26$ V vs. NHE).



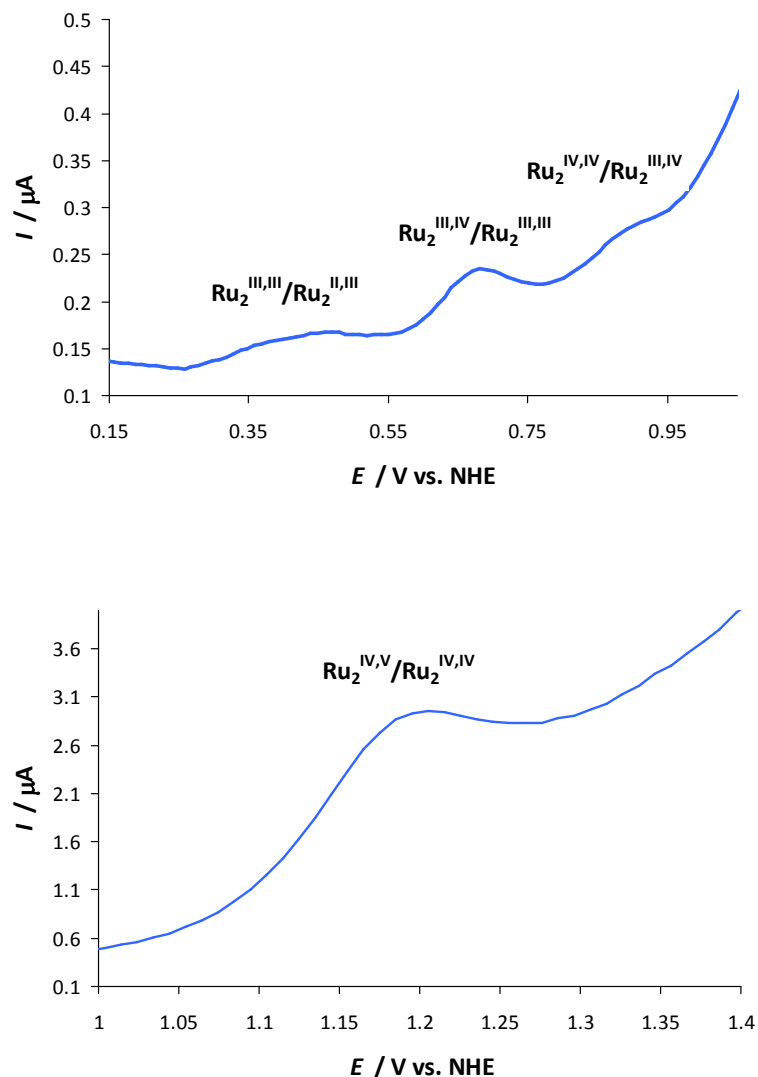


Figure S20. Differential pulse voltammogram of (—) Ru complex **3** in an aqueous phosphate buffer solution (pH 7.2). Upper: Differential pulse voltammogram of Ru complex **3** in the range $-0.2 < E < 0.2$. Middle: Differential pulse voltammogram of Ru complex **3** in the range $0.15 < E < 1.05$. Lower: Differential pulse voltammogram of Ru complex **3** in the range $1.0 < E < 1.4$. Conditions: Voltammogram was recorded in an aqueous phosphate buffer solution (0.1 M, pH 7.2) containing complex **3** (60 μM) with a scan rate of 0.1 V s^{-1} , using the $[\text{Ru}(\text{bpy})_3]^{3+}/[\text{Ru}(\text{bpy})_3]^{2+}$ couple as a standard ($E_{1/2} = 1.26 \text{ V vs. NHE}$).

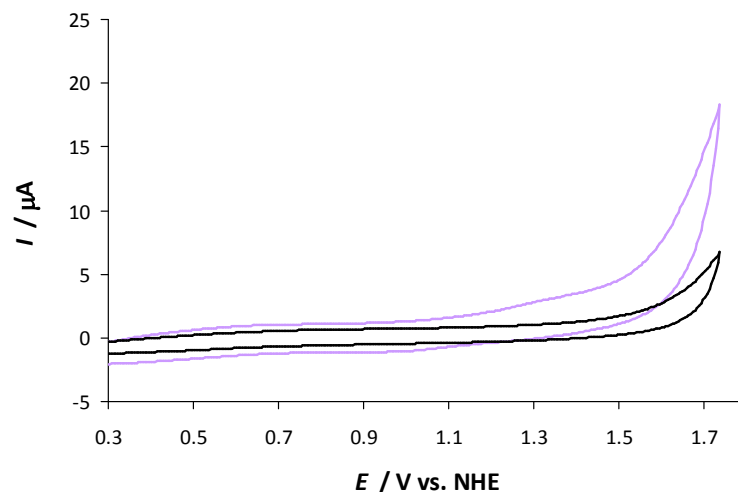


Figure S21. Cyclic voltammograms of (—) Ru complex **3** in an aqueous triflic acid solution (pH 1.0) and of (—) triflic acid (0.1 M, pH 1.0) in the absence of Ru complex **3**. Conditions: Voltammograms were recorded in an aqueous triflic acid solution (0.1 M, pH 1.0) containing complex **3** (60 μM) with a scan rate of 0.1 V s^{-1} , using the $[\text{Ru}(\text{bpy})_3]^{3+}/[\text{Ru}(\text{bpy})_3]^{2+}$ couple as a standard ($E_{1/2} = 1.26$ V vs. NHE).

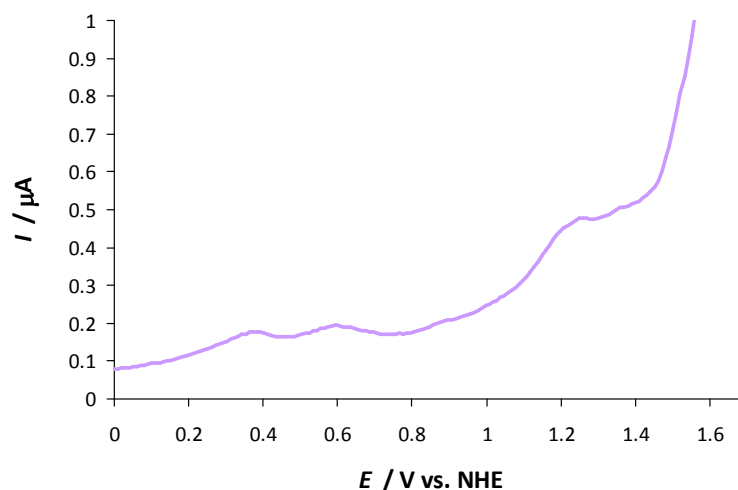


Figure S22. Differential pulse voltammogram of (—) Ru complex **3** in an aqueous triflic acid solution (pH 1.0). Conditions: Voltammogram was recorded in an aqueous triflic acid solution (0.1 M, pH 1.0) containing complex **3** (60 μM) with a scan rate of 0.1 V s^{-1} , using the $[\text{Ru}(\text{bpy})_3]^{3+}/[\text{Ru}(\text{bpy})_3]^{2+}$ couple as a standard ($E_{1/2} = 1.26$ V vs. NHE).

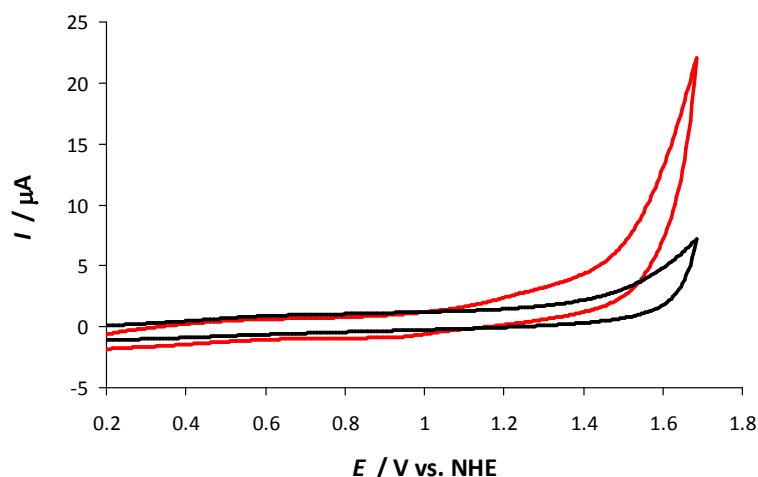


Figure S23. Cyclic voltammograms of (—) Ru complex **3** in an aqueous H_3PO_4 solution (pH 1.0) and of (—) H_3PO_4 (pH 1.0) in the absence of Ru complex **3**. Conditions: Voltammograms were recorded in an aqueous H_3PO_4 solution (0.1 M, pH 1.0) containing complex **3** (60 μM) with a scan rate of 0.1 V s^{-1} , using the $[\text{Ru}(\text{bpy})_3]^{3+}/[\text{Ru}(\text{bpy})_3]^{2+}$ couple as a standard ($E_{1/2} = 1.26$ V vs. NHE).

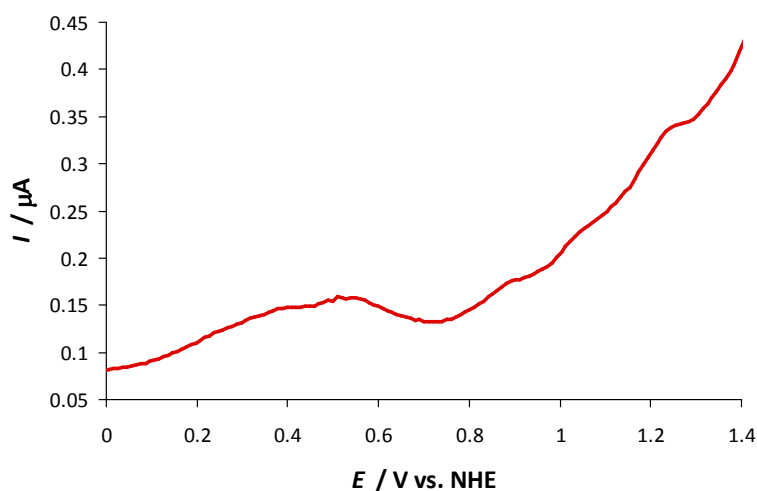


Figure S24. Differential pulse voltammogram of (—) Ru complex **3** in an aqueous H_3PO_4 solution (pH 1.0). Conditions: Voltammogram was recorded in an aqueous H_3PO_4 solution (0.1 M, pH 1.0) containing complex **3** (60 μM) with a scan rate of 0.1 V s^{-1} , using the $[\text{Ru}(\text{bpy})_3]^{3+}/[\text{Ru}(\text{bpy})_3]^{2+}$ couple as a standard ($E_{1/2} = 1.26$ V vs. NHE).

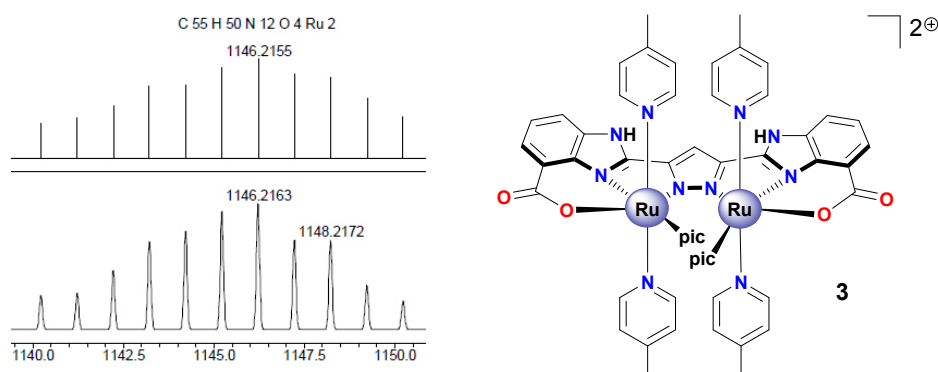


Figure S25. Upper: ESI-HRMS spectrum of the dinuclear Ru complex **3**, $[(\text{H}_2\text{L})\text{Ru}_2^{\text{II,III}}(\text{pic})_6]^{2+}$, $([(\text{H}_2\text{L})\text{Ru}_2^{\text{II,III}}(\text{pic})_6]^{2+} - \text{H}^+)^+$ recorded in positive mode. Lower: simulated spectrum.

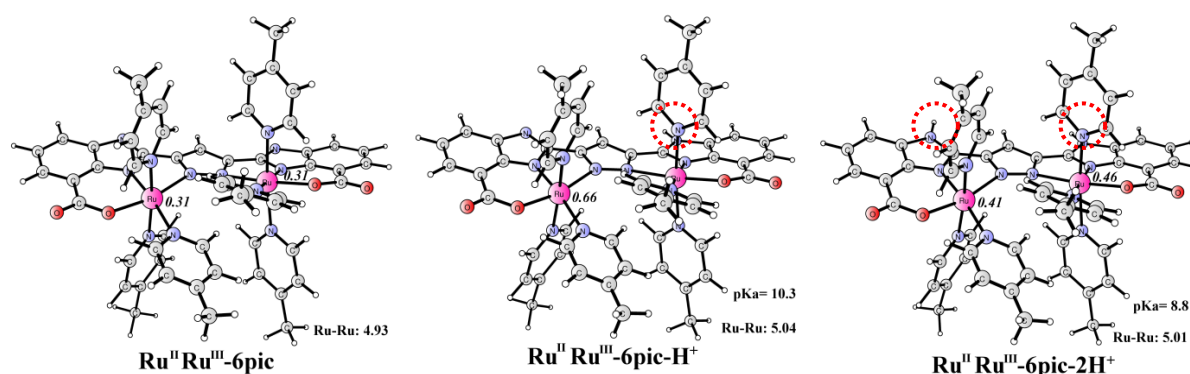


Figure S26. Optimized doublet structures of the $\text{Ru}_2^{\text{II,III}}$ complexes with six picoline ligands ($[\text{Ru}_2^{\text{II,III}}(\text{pic})_6]$) in different protonation states (total charge from left to right: 0, +1 and +2, respectively). Spin densities on Ru are shown in italic and the Ru-Ru distances are given in Ångstrom. Crucial protons are highlighted with red dotted circles.

Table S1. Cartesian coordinates for $\text{Ru}^{\text{II}}\text{Ru}^{\text{III}}\text{-6pic}$.						
Center number	Atomic number	Atomic type	Coordinates (Angstroms)			
			X	Y	Z	
1	6	0	4.504691	-0.562484	-2.051758	
2	6	0	4.507428	-0.741607	-3.468222	
3	6	0	5.743715	-0.93568	-4.097146	
4	6	0	6.893518	-0.925323	-3.29853	
5	6	0	6.854814	-0.7175	-1.902114	

6	6	0	5.644444	-0.519756	-1.235027
7	6	0	2.486324	-0.454521	-2.855327
8	6	0	5.578072	-0.241417	0.246865
9	8	0	6.604204	-0.297358	0.922287
10	8	0	4.415958	0.087856	0.803289
11	7	0	3.215509	-0.406403	-1.694441
12	7	0	3.206713	-0.664015	-3.955371
13	6	0	-0.000009	0.000024	-3.476843
14	6	0	-1.077686	0.224524	-2.624574
15	7	0	0.668337	-0.118143	-1.2972
16	7	0	-0.668349	0.118151	-1.297196
17	6	0	1.077672	-0.224484	-2.62458
18	6	0	-4.504703	0.562491	-2.051733
19	6	0	-4.507448	0.741634	-3.468196
20	6	0	-5.74374	0.935693	-4.097114
21	6	0	-6.893542	0.925289	-3.298497
22	6	0	-6.854832	0.717428	-1.902087
23	6	0	-5.644456	0.519707	-1.235004
24	6	0	-2.486339	0.454567	-2.85531
25	7	0	-3.215518	0.40643	-1.694422
26	7	0	-3.206737	0.664049	-3.955351
27	6	0	-5.578087	0.241301	0.246877
28	8	0	-6.60425	0.297055	0.922269
29	8	0	-4.415939	-0.087801	0.803328
30	44	0	-2.462614	-0.065713	0.046952
31	44	0	2.462623	0.065727	0.046941
32	6	0	-3.201956	2.474974	1.551282
33	6	0	-1.758598	2.908472	-0.196089
34	6	0	-3.29871	3.827701	1.852907
35	6	0	-1.812364	4.274321	0.049019
36	6	0	-2.597354	4.773433	1.094956
37	6	0	-3.628098	-2.854399	0.19377
38	6	0	-1.998096	-2.761131	-1.436179
39	6	0	-3.885979	-4.1892	-0.090571
40	6	0	-2.208764	-4.092443	-1.774883
41	6	0	-3.174712	-4.847489	-1.100292
42	6	0	3.202018	-2.47496	1.55125
43	6	0	1.758632	-2.908457	-0.1961
44	6	0	3.298783	-3.827687	1.852868
45	6	0	1.812408	-4.274307	0.049002
46	6	0	2.597417	-4.77342	1.094925
47	6	0	3.628078	2.854426	0.193753
48	6	0	1.998043	2.761159	-1.436162
49	6	0	3.885943	4.189232	-0.090582
50	6	0	2.208695	4.092476	-1.774861
51	6	0	3.174651	4.847524	-1.100284
52	6	0	-2.699091	-0.828101	3.03497
53	6	0	-0.645826	-1.434537	2.182856
54	6	0	-2.413839	-1.438024	4.251354
55	6	0	-0.299024	-2.077465	3.365494
56	6	0	-1.190012	-2.089298	4.445215
57	6	0	2.699113	0.828095	3.034963
58	6	0	0.645843	1.434537	2.182861
59	6	0	2.413862	1.43801	4.251355
60	6	0	0.299045	2.077455	3.365502

61	6	0	1.190038	2.089279	4.445224
62	7	0	2.690307	2.13421	-0.461645
63	7	0	2.432786	-2.002019	0.545172
64	7	0	1.82736	0.809266	2.002505
65	7	0	-1.82734	-0.809265	2.002506
66	7	0	-2.432745	2.002034	0.545189
67	7	0	-2.690334	-2.134185	-0.46164
68	1	0	-5.809212	1.080548	-5.171425
69	1	0	-7.860247	1.071823	-3.772901
70	1	0	-7.770924	0.696996	-1.321101
71	1	0	-0.00001	0.000031	-4.555608
72	1	0	5.809182	-1.080523	-5.171459
73	1	0	7.860218	-1.071873	-3.772937
74	1	0	7.770906	-0.697123	-1.321126
75	1	0	-1.160104	2.50311	-1.00091
76	1	0	-3.777284	1.733647	2.090025
77	1	0	-3.941334	4.13792	2.671433
78	1	0	-1.239314	4.944133	-0.584745
79	1	0	-4.195147	-2.311601	0.940362
80	1	0	-1.262975	-2.166728	-1.961106
81	1	0	-4.657529	-4.705631	0.472547
82	1	0	-1.621131	-4.529227	-2.576897
83	1	0	3.941423	-4.137905	2.671381
84	1	0	1.239351	-4.94412	-0.584754
85	1	0	1.160123	-2.503095	-1.00091
86	1	0	3.777352	-1.733633	2.089987
87	1	0	4.195147	2.311626	0.940327
88	1	0	1.262915	2.166757	-1.961077
89	1	0	4.657499	4.705665	0.472526
90	1	0	1.621042	4.529261	-2.576859
91	1	0	-3.6644	-0.374873	2.835227
92	1	0	0.040268	-1.396013	1.347087
93	1	0	-3.159868	-1.412957	5.040444
94	1	0	0.670287	-2.561488	3.435673
95	1	0	3.664423	0.374871	2.835214
96	1	0	-0.040252	1.396019	1.347093
97	1	0	3.159893	1.412939	5.040443
98	1	0	-0.670267	2.561479	3.435687
99	6	0	2.713467	-6.250357	1.365842
100	1	0	3.557351	-6.675898	0.809218
101	1	0	2.889044	-6.450634	2.426591
102	1	0	1.812585	-6.786883	1.055371
103	6	0	-3.461874	-6.279694	-1.467747
104	1	0	-4.24701	-6.327478	-2.232136
105	1	0	-2.577081	-6.774435	-1.877951
106	1	0	-3.81211	-6.852188	-0.60424
107	6	0	3.461794	6.279734	-1.467732
108	1	0	4.246916	6.327531	-2.232134
109	1	0	2.57699	6.774471	-1.877917
110	1	0	3.812039	6.852225	-0.604227
111	6	0	-2.713393	6.25037	1.365876
112	1	0	-1.812449	6.78687	1.055537
113	1	0	-3.557182	6.675949	0.809137
114	1	0	-2.88911	6.450641	2.426603
115	6	0	0.861805	2.794457	5.735808

116	1	0	1.407879	2.361528	6.57847
117	1	0	1.136656	3.854948	5.677948
118	1	0	-0.20864	2.747314	5.956019
119	6	0	-0.861796	-2.794491	5.735795
120	1	0	-1.407321	-2.361088	6.578572
121	1	0	-1.137359	-3.854812	5.678189
122	1	0	0.208748	-2.747998	5.955649

Table S2. Cartesian coordinates for Ru^{II}Ru^{III}-6pic-H⁺.

Center number	Atomic number	Atomic type	Coordinates (Angstroms)		
			X	Y	Z
1	6	0	-4.577135	0.592053	-2.062141
2	6	0	-4.581449	0.71215	-3.474956
3	6	0	-5.802851	0.918013	-4.114942
4	6	0	-6.955507	0.981084	-3.312837
5	6	0	-6.918637	0.833933	-1.915036
6	6	0	-5.706885	0.623597	-1.243255
7	6	0	-2.552007	0.386108	-2.876515
8	6	0	-5.634687	0.413757	0.248026
9	8	0	-6.644419	0.533792	0.930985
10	8	0	-4.472095	0.073121	0.806701
11	7	0	-3.280286	0.406078	-1.699524
12	7	0	-3.270876	0.571007	-3.96487
13	6	0	-0.067105	-0.104037	-3.493422
14	6	0	1.005165	-0.303497	-2.622688
15	7	0	-0.733638	0.06883	-1.327284
16	7	0	0.60327	-0.167009	-1.306629
17	6	0	-1.142854	0.140269	-2.645172
18	6	0	4.485187	-0.65463	-2.134689
19	6	0	4.511945	-0.871875	-3.527994
20	6	0	5.722088	-1.096674	-4.185061
21	6	0	6.871778	-1.080759	-3.39013
22	6	0	6.832568	-0.842518	-2.00164
23	6	0	5.629608	-0.613683	-1.331603
24	6	0	2.413898	-0.535971	-2.825796
25	7	0	3.183662	-0.470859	-1.753222
26	7	0	3.176928	-0.78751	-3.940532
27	6	0	5.601801	-0.317165	0.160023
28	8	0	6.657859	-0.383089	0.781527
29	8	0	4.469131	0.021278	0.743529
30	44	0	2.495629	0.030338	0.050328
31	44	0	-2.539881	-0.004968	0.023861
32	6	0	3.23859	-2.513205	1.564465
33	6	0	1.698017	-2.941019	-0.093579
34	6	0	3.307244	-3.860465	1.896652
35	6	0	1.720676	-4.3024	0.182627
36	6	0	2.540804	-4.803684	1.200677
37	6	0	3.698668	2.8047	0.203099
38	6	0	2.098128	2.724112	-1.452598
39	6	0	3.97774	4.134823	-0.083129
40	6	0	2.32961	4.051437	-1.794995

41	6	0	3.293543	4.799409	-1.10816
42	6	0	-3.179448	2.599441	1.469703
43	6	0	-1.590587	2.91565	-0.18043
44	6	0	-3.182225	3.954774	1.772977
45	6	0	-1.549717	4.280089	0.067759
46	6	0	-2.359598	4.840131	1.064997
47	6	0	-3.829147	-2.741174	0.276458
48	6	0	-2.137578	-2.801227	-1.296442
49	6	0	-4.133316	-4.07686	0.050771
50	6	0	-2.394928	-4.136823	-1.575331
51	6	0	-3.417604	-4.814915	-0.899824
52	6	0	2.808667	0.733204	3.032294
53	6	0	0.775416	1.432696	2.210876
54	6	0	2.555795	1.32966	4.262962
55	6	0	0.461508	2.06493	3.407247
56	6	0	1.359509	2.022174	4.481729
57	6	0	-2.748311	-0.687279	3.039744
58	6	0	-0.703142	-1.329014	2.178999
59	6	0	-2.450704	-1.260299	4.269205
60	6	0	-0.347359	-1.940149	3.375388
61	6	0	-1.226994	-1.915261	4.464472
62	7	0	-2.839216	-2.098373	-0.383003
63	7	0	-2.386984	2.071094	0.510346
64	7	0	-1.885997	-0.708149	1.999262
65	7	0	1.929947	0.764857	2.005666
66	7	0	2.436702	-2.034626	0.584482
67	7	0	2.764388	2.088552	-0.46486
68	1	0	5.779885	-1.270329	-5.254661
69	1	0	7.833421	-1.250494	-3.864185
70	1	0	7.747153	-0.82435	-1.419037
71	1	0	-0.082945	-0.121882	-4.57292
72	1	0	-5.86468	1.01918	-5.193701
73	1	0	-7.91621	1.140105	-3.793219
74	1	0	-7.83113	0.872144	-1.329867
75	1	0	1.066155	-2.538039	-0.874332
76	1	0	3.863505	-1.782787	2.060206
77	1	0	3.978807	-4.169282	2.692118
78	1	0	1.095175	-4.968863	-0.403559
79	1	0	4.246001	2.264182	0.965259
80	1	0	1.358166	2.139087	-1.98317
81	1	0	4.744311	4.644182	0.492955
82	1	0	1.759741	4.493122	-2.607333
83	1	0	-3.846302	4.316352	2.551801
84	1	0	-0.882455	4.901467	-0.520846
85	1	0	-0.973735	2.461873	-0.94444
86	1	0	-3.845615	1.905678	1.965916
87	1	0	-4.393689	-2.139157	0.97794
88	1	0	-1.356906	-2.265475	-1.819219
89	1	0	-4.94341	-4.531732	0.612123
90	1	0	-1.800125	-4.6412	-2.330629
91	1	0	3.756824	0.252711	2.820263
92	1	0	0.086087	1.445939	1.377238
93	1	0	3.307959	1.26272	5.043358
94	1	0	-0.486516	2.587179	3.494538
95	1	0	-3.710631	-0.228261	2.839529

96	1	0	-0.023703	-1.316747	1.33607
97	1	0	-3.184596	-1.20633	5.067604
98	1	0	0.620085	-2.426231	3.450682
99	6	0	-2.373317	6.319975	1.33608
100	1	0	-3.150719	6.806269	0.734373
101	1	0	-2.593491	6.533174	2.38537
102	1	0	-1.418818	6.785003	1.07641
103	6	0	3.604355	6.226866	-1.472445
104	1	0	4.46939	6.269565	-2.145213
105	1	0	2.765776	6.703862	-1.986444
106	1	0	3.853681	6.819834	-0.587957
107	6	0	-3.754891	-6.24944	-1.203697
108	1	0	-4.565819	-6.298418	-1.940405
109	1	0	-2.898892	-6.785158	-1.621728
110	1	0	-4.09653	-6.777867	-0.309589
111	6	0	2.62364	-6.2752	1.507956
112	1	0	1.729561	-6.807387	1.172831
113	1	0	3.485204	-6.724147	0.999205
114	1	0	2.752824	-6.453377	2.579293
115	6	0	-0.891318	-2.583211	5.771167
116	1	0	-1.297754	-2.026198	6.619851
117	1	0	-1.324558	-3.590159	5.807432
118	1	0	0.188652	-2.68407	5.90517
119	6	0	1.069164	2.714304	5.787502
120	1	0	1.594927	2.23762	6.618939
121	1	0	1.398096	3.760003	5.750055
122	1	0	-0.001588	2.717628	6.01025
123	1	0	2.832546	-0.896701	-4.881543

Table S3. Cartesian coordinates for Ru^{II}Ru^{III}-6pic-2H⁺.

Center number	Atomic number	Atomic type	Coordinates (Angstroms)		
			X	Y	Z
1	6	0	4.549287	-0.59098	-2.10197
2	6	0	4.610068	-0.76399	-3.49842
3	6	0	5.836074	-0.98393	-4.12768
4	6	0	6.961186	-1.00901	-3.29837
5	6	0	6.887804	-0.815	-1.9029
6	6	0	5.668292	-0.59091	-1.26391
7	6	0	2.496024	-0.42492	-2.84678
8	6	0	5.582234	-0.34258	0.225717
9	8	0	6.585994	-0.46196	0.909963
10	8	0	4.424188	0.032262	0.771626
11	7	0	3.24222	-0.40399	-1.74991
12	7	0	3.285046	-0.64831	-3.94392
13	6	0	0.012296	0.004629	-3.50633
14	6	0	-1.0655	0.204613	-2.64492
15	7	0	0.679249	-0.09505	-1.32219
16	7	0	-0.6556	0.10592	-1.32189
17	6	0	1.089965	-0.19535	-2.64654
18	6	0	-4.53067	0.585739	-2.11855
19	6	0	-4.582	0.761475	-3.51528

20	6	0	-5.80385	0.97754	-4.154
21	6	0	-6.93553	0.995794	-3.33384
22	6	0	-6.87198	0.798602	-1.93833
23	6	0	-5.65685	0.57878	-1.28979
24	6	0	-2.47168	0.429964	-2.84904
25	7	0	-3.22498	0.40307	-1.75681
26	7	0	-3.25394	0.65239	-3.95157
27	6	0	-5.58484	0.32612	0.200782
28	8	0	-6.59999	0.431229	0.871369
29	8	0	-4.43018	-0.03409	0.758382
30	44	0	-2.50549	-0.04387	0.037587
31	44	0	2.508484	0.045256	0.038703
32	6	0	-3.22793	2.527661	1.516154
33	6	0	-1.70541	2.932009	-0.1699
34	6	0	-3.29564	3.878949	1.826152
35	6	0	-1.72743	4.296245	0.085288
36	6	0	-2.53961	4.812627	1.104119
37	6	0	-3.70989	-2.81769	0.291986
38	6	0	-2.1082	-2.80204	-1.36848
39	6	0	-3.99423	-4.15444	0.052642
40	6	0	-2.34551	-4.13872	-1.66282
41	6	0	-3.3138	-4.85814	-0.95045
42	6	0	3.206241	-2.52618	1.528071
43	6	0	1.70222	-2.92771	-0.17612
44	6	0	3.266956	-3.87728	1.839451
45	6	0	1.717247	-4.29165	0.08089
46	6	0	2.516591	-4.80935	1.109115
47	6	0	3.715945	2.818188	0.300615
48	6	0	2.11808	2.807215	-1.36421
49	6	0	4.000975	4.155644	0.065422
50	6	0	2.355907	4.144513	-1.65377
51	6	0	3.323148	4.861893	-0.93737
52	6	0	-2.77101	-0.68696	3.04511
53	6	0	-0.74662	-1.39471	2.199674
54	6	0	-2.49641	-1.26071	4.279631
55	6	0	-0.41215	-2.00486	3.402031
56	6	0	-1.29344	-1.94843	4.489513
57	6	0	2.753882	0.695279	3.04708
58	6	0	0.730244	1.390373	2.188478
59	6	0	2.469425	1.270207	4.278528
60	6	0	0.386089	2.001613	3.387757
61	6	0	1.261547	1.952359	4.479984
62	7	0	2.782578	2.132421	-0.4014
63	7	0	2.429436	-2.03573	0.533208
64	7	0	1.895886	0.738188	2.002031
65	7	0	-1.90761	-0.73617	2.004941
66	7	0	-2.43769	2.037925	0.531576
67	7	0	-2.77434	-2.12975	-0.40545
68	1	0	-5.88513	1.120214	-5.22625
69	1	0	-7.90504	1.160644	-3.79244
70	1	0	-7.77693	0.807366	-1.34061
71	1	0	0.011516	0.003747	-4.58656
72	1	0	5.925582	-1.12453	-5.19952
73	1	0	7.933501	-1.17713	-3.74975
74	1	0	7.788202	-0.82989	-1.29845

75	1	0	-1.08056	2.520962	-0.95186
76	1	0	-3.84295	1.805163	2.034741
77	1	0	-3.95823	4.199489	2.624087
78	1	0	-1.10959	4.954879	-0.51682
79	1	0	-4.25219	-2.25166	1.038412
80	1	0	-1.3632	-2.24198	-1.91814
81	1	0	-4.76172	-4.63981	0.647443
82	1	0	-1.77771	-4.61333	-2.45735
83	1	0	3.919236	-4.19915	2.645284
84	1	0	1.103669	-4.94891	-0.52695
85	1	0	1.086771	-2.51561	-0.96482
86	1	0	3.815808	-1.80472	2.054504
87	1	0	4.255443	2.250768	1.047997
88	1	0	1.373645	2.249106	-1.91639
89	1	0	4.766443	4.639697	0.663792
90	1	0	1.788825	4.621599	-2.44731
91	1	0	-3.72303	-0.21047	2.844881
92	1	0	-0.06825	-1.42167	1.357027
93	1	0	-3.23546	-1.18195	5.071076
94	1	0	0.538221	-2.52274	3.483857
95	1	0	3.70912	0.222421	2.853622
96	1	0	0.055547	1.410784	1.342758
97	1	0	3.204284	1.19684	5.07439
98	1	0	-0.56762	2.514193	3.463045
99	6	0	2.593469	-6.28337	1.395427
100	1	0	3.495727	-6.70956	0.940547
101	1	0	2.652848	-6.47858	2.469715
102	1	0	1.732907	-6.81983	0.989075
103	6	0	-3.6298	-6.29589	-1.25774
104	1	0	-4.57237	-6.3663	-1.81344
105	1	0	-2.85072	-6.762	-1.86521
106	1	0	-3.75476	-6.87951	-0.34106
107	6	0	3.641108	6.299393	-1.24318
108	1	0	4.544551	6.363102	-1.86154
109	1	0	2.831101	6.786229	-1.7913
110	1	0	3.837046	6.867141	-0.32939
111	6	0	-2.62399	6.286865	1.387753
112	1	0	-1.75138	6.822581	1.00667
113	1	0	-3.51178	6.713665	0.905741
114	1	0	-2.71499	6.482772	2.459619
115	6	0	0.943112	2.620403	5.789974
116	1	0	1.267976	2.009885	6.63718
117	1	0	1.468375	3.57999	5.865825
118	1	0	-0.12632	2.818858	5.893167
119	6	0	-0.98544	-2.61643	5.802079
120	1	0	-1.34078	-2.01908	6.646249
121	1	0	-1.48888	-3.58883	5.861803
122	1	0	0.086208	-2.79095	5.92496
123	1	0	-2.93276	0.740971	-4.90381
124	1	0	2.970171	-0.73254	-4.89882

References

-
- S1 E. Dulière, M. Devillers and J. Marchand-Brynaert, *Organometallics* 2003, **22**, 804-811.
- S2 R. E. DeSimone and R. S. Drago, *J. Am. Chem. Soc.* 1970, **92**, 2343-2352.
- S3 M. J. Frisch, G. W. Trucks, H. B. Schlegel, G. E. Scuseria, M. A. Robb, J. R. Cheeseman, G. Scalmani, V. Barone, B. Mennucci, G. A. Petersson, *et. al.* Gaussian 09, Revision B.01, Gaussian, Inc., Wallingford CT, **2009**.
- S4 A. D. Becke, *J. Chem. Phys.* 1993, **98**, 5648-5652.
- S5 D. Andrae, U. Häußermann, M. Dolg, H. Stoll and H. Preuß, *Theor. Chim. Acta.* 1990, **77**, 123-141.
- S6 A. V. Marenich, C. J. Cramer and D. G. Truhlar, *J. Phys. Chem. B* 2009, 113, 6378-6396.
- S7 M. Reiher, O. Salomon and B. A. Hess, *Theor. Chem. Acc.* 2001, **107**, 48-55.
- S8 D. M. Camaioni and C. A. Schwerdtfeger, *J. Phys. Chem. A* 2005, 109, 10795-10797.
- S9 S. Grimme, *J. Comput. Chem.* 2006, **27**, 1787-1799.
- S10 V. J. Arán, M. Kumar, J. Molina, L. Lamarque, P. Navarro, E. García-España, J. A. Ramírez, S. V. Luis and B. Escuder, *J. Org. Chem.* 1999, **64**, 6135-6146.